Mon. Not. R. Astron. Soc. **000**, 1–11 (2010) Printed 9 November 2010 (MN LATEX style file v2.2)

Eurybates and Ennomos — the only asteroid families among Trojans?

M. Brož[1⋆] and J. Rozehnal[1]
[1] *Institute of Astronomy, Charles University, Prague, V Holešovičkách 2, 18000 Prague 8, Czech Republic*

Accepted ???. Received ???; in original form ???

ABSTRACT
We study orbital and physical properties of Trojan asteroids of Jupiter. We try to discern all families previously discussed in literature, but we conclude there is only one significant family among Trojans, namely the cluster around asteroid (3548) Eurybates. It is the only cluster, which has all of the following characteristics: (i) it is clearly concentrated in the proper-element space; (ii) size-frequency distribution is different from background asteroids; (iii) we have a reasonable collisional/dynamical model of the family. Henceforth, we can consider it as a real collisional family.

We also report a discovery of the Ennomos family. The asteroid (4709) Ennomos is known to have a very high albedo $p_V \simeq 0.15$, which may be related to a hypothetical cratering event which exposed ice (Fernández et al. 2003). The relation between the collisional family and the exposed surface of the parent body is a unique opportunity to study the physics of cratering events.

Key words: celestial mechanics – minor planets, asteroids – methods: N-body simulations.

1 INTRODUCTION

Trojans of Jupiter, which reside in the neighbourhood of L_4 and L_5 Lagrangian points, serve as an important test of the planetary migration theory (Morbidelli et al. 2005). Their inclination distribution, namely the large spread of I, can be explained as a result of chaotic capture during a brief period when Jupiter and Saturn encountered a 1:2 mean-motion resonance. Moreover, the Late Heavy Bombardment provides the timing of this resonant encounter $\simeq$3.8 Gyr ago (Gomes et al. 2005). It is thus important to understand the population of Trojans accurately.

There are several unresolved problems regarding Trojans, however, for example the number of families, which is a stringent constraint for collisional models. As many as ten families were studied by Roig et al. (2008), using relatively sparse SLOAN data and spectra. They noted most families seem to be heterogeneous from the spectroscopic point of view, with one exception — the C-type Eurybates family. As we argue in this paper, the number of families (with parent-body size $D \gtrsim 100$ km) is indeed as low as one.

Another strange fact is the ratio of L_4 and L_5 Trojans. Szabó et al. (2007) used SLOAN colour data to reach fainter than orbital catalogues and estimated the ratio to $N(L_4)/N(L_5) = 1.6 \pm 0.1$. There is no clear explanation for this, since the chaotic capture as a gravitational interaction should be independent of size or L_4/L_5 membership. Any hypothesis involving collisions would require a relatively recent disruption of a huge parent body, which is highly unlikely (O'Brien and Morbidelli 2008). This is again related to the actual observed number of Trojan families.

Brož and Vokrouhlický (2008) studied another resonant population, the so called Hilda group in the 3/2 mean-motion resonance with Jupiter, and reported only two families: Hilda and Schubart with approximately 200 and 100 km parent bodies. This number might be in accord with low collisional probabilities, assuming the Hilda family is very old and experienced the Late Heavy Bombardment (Brož et al. 2010).

Levison et al. (2009) compared the observed distribution of D-type asteroids and the model of their delivery from transneptunian region. They found a good match assuming the D-types (presumably of cometary origin) are easy-to-disrupt objects (with the strength more than 5 times lower than that of solid ice). Note that Trojan asteroids are a mixture of C- and D-type objects and we have to discriminate between them with respect to collisional behaviour.

All of the works mentioned above are a good motivation for us to focus on asteroid families in the Trojan population. The paper is organised as follows. First, we describe our data sources and methods in Section 2. A detailed study of orbital and physical properties of families (and other 'false' groupings) is a matter of Section 3. Section 4 is devoted

⋆ E-mail: mira@sirrah.troja.mff.cuni.cz (MB)

to the modelling of long-term dynamical evolution. Finally, there are concluding remarks in Section 5.

2 METHODS

2.1 Resonant elements

We use the symplectic SWIFT integrator (Levison & Duncan 1994) for orbital calculations. Our modifications include a second order scheme of Laskar & Robutel (2001) and online digital filters, which enable us to compute suitable resonant proper elements: libration amplitude $d \equiv a - a'$, where a is the osculating semimajor axis of an asteroid and a' that of Jupiter, eccentricity e, inclination $\sin I$. (In figures, we usually plot a mean value $\bar{a}$ of semimajor axis plus the libration amplitude d.) We employ their definition from Milani (1993). The source of initial osculating elements is the AstOrb catalogue, version JD = 2455000.5 (Jun 18th 2009).

There are actually two independent filters running in parallel: in the first one, we sample osculating elements every 1 yr, compute mean elements using the filter sequence B, B with decimation factors 3, 3 (refer to Quinn, Tremain & Duncan 1991) a store this data in a buffer spanning 1 kyr. We then estimate the libration frequency f by a linear fit of $\phi(t) = \lambda - \lambda' - \chi$, where λ, λ' are the mean longitudes of an asteroid and Jupiter and $\chi = \pm 60^\circ$ for L_4 or L_5 respectively. The revolution of angle $\phi(t)$ must not be confined to the interval $[0, 360^\circ)$, of course. The amplitude of d is computed for the already known f by a discrete Fourier transform. Finally, an off-line running-average filter with a window 1 Myr is used to smooth the data.[1]

In the second filter, we compute proper eccentricity and proper inclination by sampling osculating elements (1 yr step), computing mean elements using a filter sequence A, A, B and decimation factors 10, 10, 3, and then we apply a frequency modified Fourier transform (Nesvorný & Šidlichovský 1997), which gives us the relevant proper amplitudes.

The values of the resonant elements agree very well with those listed in the AstDyS catalogue by Knežević & Milani (see Figure 1). There are only few outliers, probably due to a different time span of integration. We computed proper elements for 1789 L_4 and 1352 L_5 Trojan asteroids.[2] This sample is roughly twice larger than previously analysed. The ratio of populations valid for bright ($H \lesssim 15$ mag) asteroids is thus $N(L_4)/N(L_5) \simeq 1.3$.

The overall distribution of Trojans in the $(d, e, \sin I)$ space is shown in Figure 2. Note there is only one cluster visible immediately in the bottom-left panel — around (3548) Eurybates. The reason is its tight confinement in inclinations ($\sin I = 0.125$ to 0.135).

[1] Equivalently, we may compute the amplitude in mean longitudes $D \equiv \lambda - \lambda'$. Anyway, there is a linear relation between d and D.

[2] The data are available in an electronic form on our web site `http://sirrah.troja.mff.cuni.cz/~mira/mp/`. We use also one-apparition orbits for the purposes of physical studies. Of course, orbital studies require more precise multi-apparition data.

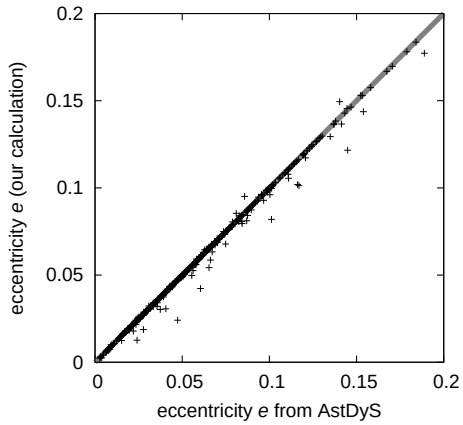

Figure 1. Comparison of the resonant eccentricity calculated by our code to that of Knežević & Milani (AstDyS catalogue). There is a line $x = y$ to aid a comparison.

2.2 Hierarchical clustering

In order to detect clusters in the resonant element space we use a hierarchical clustering method (Zappalá et al. 1994) with a standard metric d_1, with δa substituted by d. We run the HCM code many times with various starting bodies and different cut–off velocities $v_{\rm cutoff}$ and determine the number of bodies N in the given cluster. We find the $N(v_{\rm cutoff})$ dependence a very useful diagnostic tool. We can see these dependences for L_4 and L_5 Trojans in Figure 3.

It is easy to recognise, if a cluster has a concentration towards the centre — even at low $v_{\rm cutoff}$ it must have more than one member ($N \gg 1$). It is also instructive to compare clusters with a random background (thin lines), which we generated artificially by a random-number generator in the same volume of the (d, e, I) space. Insignificant (random) clusters usually exhibit an abrupt increase of N at a high cut–off velocity.

As starting bodies we selected those listed in Roig et al. (2008). Only three clusters, namely the Eurybates, Aneas, 1998 RG_{10} seem to be somewhat concentrated, i.e., denser than the background. The Hektor cluster is also concentrated but it contains only a relatively low number of members (20 to 70) before it merges with the background. In other words, smaller asteroids do not seem concentrated around (624) Hektor. Remaining clusters are more or less comparable to the background.

Nevertheless, we report a detection of a previously unknown cluster around (4709) Ennomos in L_5. It is relatively compact, since the minimum cut-off velocity is 70 m/s only. The cluster contains mostly small bodies which were discovered only recently.

Finally, let us point out a very tight cluster around (9799) 1996 RJ, associated already at $v_{\rm cutoff} = 20$ m/s. It is located at high inclinations and contains 9 bodies, three of them having short arcs. The cluster seems peculiar in the osculating element space too since it exhibits a non-random distribution of nodes and perihelia (see Table 1). This is similar to very young families like the Datura (Nesvorný et al. 2006) and it makes the 1996 RJ cluster a particularly interesting case with respect to collisional dynamics. Because one has to use slightly different methods for studies of such

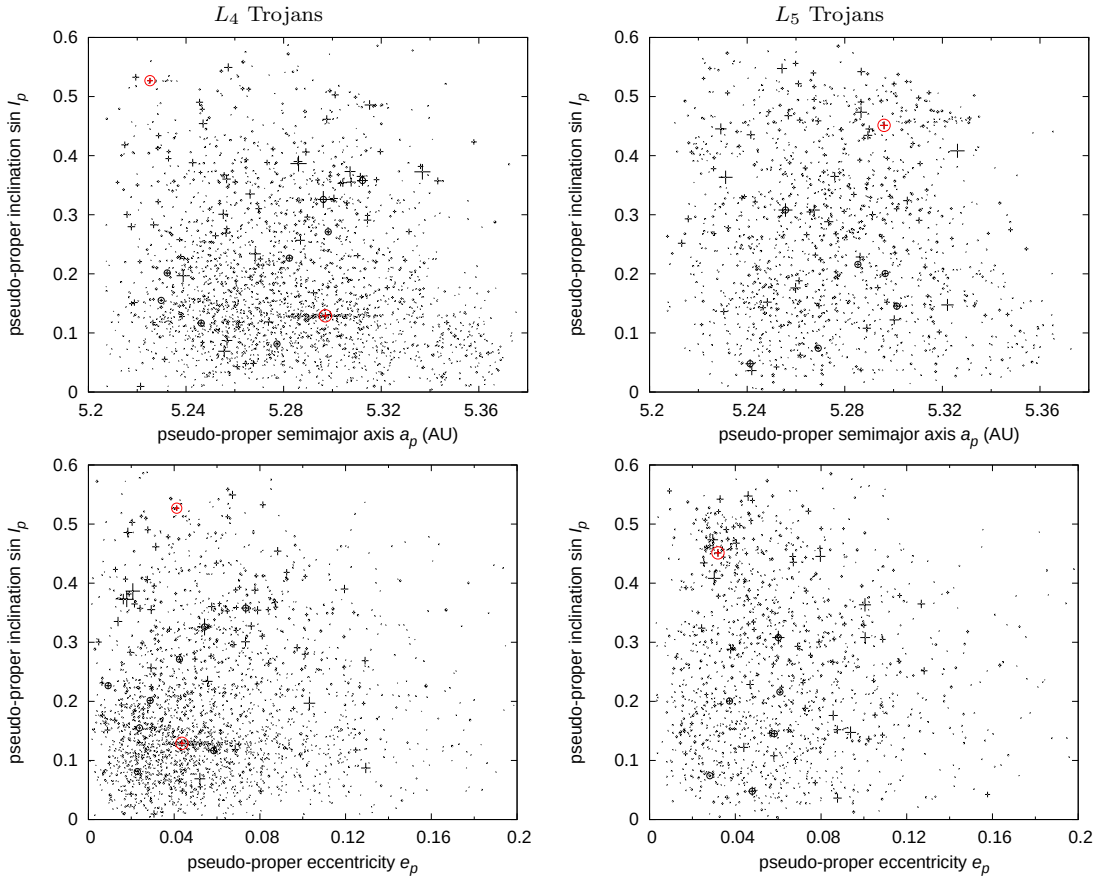

Figure 2. The resonant elements $(a \equiv \bar{a} + d, \sin I)$ and $(e, \sin I)$ for L_4 and L_5 Trojans. The crosses indicate relative sizes of bodies, taken either from the AstOrb catalogue or computed from absolute magnitude H and geometric albedo p_V. In this plot, we assumed $p_V = 0.058$ for L_4 Trojans and 0.045 for those in L_5 (it corresponds to medians of known p_V's). The asteroids (3548) Eurybates, (9799) 1996 RJ in L_4 and (4709) Ennomos in L_5, around which significant clusters are visible, are shown in red.

Table 1. List of nine members of the (9799) 1996 RJ cluster and their proper $(a, e, \sin I)$ and osculating $(\Omega_{\rm osc}, \varpi_{\rm osc})$ elements and absolute magnitude H. Note the distribution of nodes and perihelia is not entirely uniform. Asteroids with short-arc orbits (<60 days) are denoted by a * symbol.

number	designation		a	e	$\sin I$	$\Omega_{\rm osc}$	$\varpi_{\rm osc}$	H/mag
9799	1996 RJ		5.2252	0.0412	0.5269	115.4	259.6	9.9
89938	2002 FR_4		5.2324	0.0394	0.5274	70.0	23.1	12.5
226027	2002 EK_{127}		5.2316	0.0399	0.5263	62.8	352.9	12.6
243316	2008 RL_{32}		5.2340	0.0398	0.5268	27.3	358.2	12.8
	2005 MG_{24}		5.2275	0.0404	0.5252	172.3	236.5	13.1
	2008 OW_{22}	*	5.2276	0.0401	0.5274	53.7	340.9	13.9
	2009 RA_{17}	*	5.2258	0.0409	0.5272	257.7	194.5	13.7
	2009 RK_{63}	*	5.2305	0.0407	0.5260	56.4	5.6	12.8
	2009 SR_{30}		5.2362	0.0409	0.5258	103.6	22.0	13.3

young families we postpone a detailed analysis to a next paper.

Let us compare Trojan clusters to the well known asteroid families in the outer Main Belt (Figure 4). Most families (e.g., Themis, Koronis, Eos) exhibit a steady increase of N until they merge with another families or the entire outer Main Belt. Eurybates is the only Trojan family which behaves in a similar fashion. The Veritas family (dynamically young, Nesvorný et al. 2003) exhibits a different behaviour — for a large interval of $v_{\rm cutoff}$ the number of members N remains almost the same, which indicates a clear separation from the background population. With respect to the $N(v_{\rm cutoff})$ dependence, the Ennomos family is similar to Veritas.

2.3 Size-frequency distribution

At first, let us assume a single value of albedo for all family members. It is a reasonable assumption if the family is of collisional origin. We can then calculate sizes from absolute

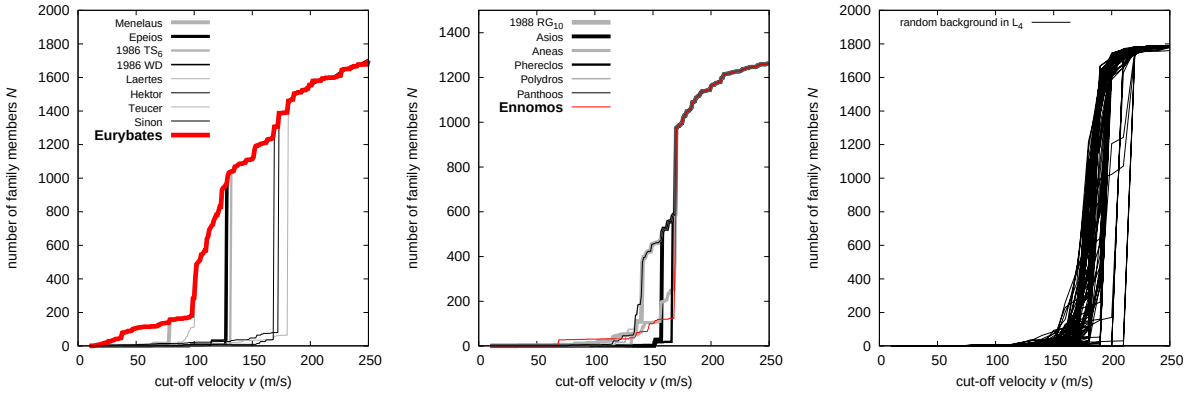

Figure 3. Left panel: The dependence of the number of family members N on the cut–off velocity $v_{\rm cutoff}$ computed by the hierarchical clustering method. Only clusters among L_4 Trojans are included in this plot. Middle panel: The same $N(v_{\rm cutoff})$ dependence for L_5 Trojans. Right panel: Artificial clusters selected from *random* distribution of asteroids generated in the same volume of the $(d, e, \sin I)$ space.

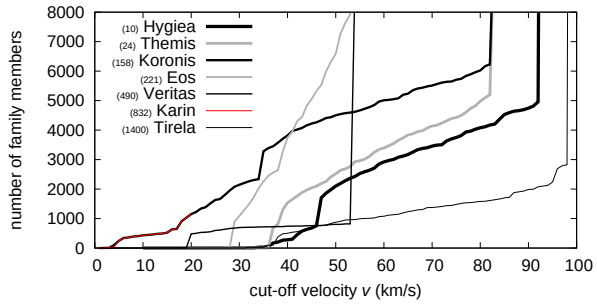

Figure 4. The $N(v_{\rm cutoff})$ dependence for seven outer main-belt families. If we would consider only a subset of asteroids brighter than $H = 15$ mag, which is an approximate observational limit for Trojans, the $N(v_{\rm cutoff})$ dependencies would be qualitatively the same, only slightly shifted to larger cut–off velocities.

magnitudes and construct size-frequency distributions. Figure 5 shows a comparison of SFD's for the clusters detected by the HCM[3] and for the whole population of L_4 and L_5 Trojans.

A slope γ of the cumulative distribution $N(>D) \propto D^{\gamma}$ is an indicative parameter. For L_4 and L_5 Trojans it equals to -2.0 ± 0.1 and -1.9 ± 0.1 in the intermediate size range 15 to 60 km. It is steeper at large sizes. The uncertainties are mainly due to a freedom in selection of the size range and the difference between L_4 and L_5 SFD's does not seem significant. The clusters have typically similar slope as background (within 0.1 uncertainty), thought sometimes the results are inconclusive due to small number of members. The Eurybates family with -2.5 ± 0.1 slope is on the other hand significantly steeper than the mean slope of the whole Trojan population.[4] There are two more groups which exhibit a relatively steep slope, namely Laertes in L_4 ($\gamma = -3.1$) and 1988 RG_{10} in L_5 ($\gamma = -2.6$).

We should be aware, however, that even the background exhibits a trend with respect to inclinations (see Figure 6). Slope γ typically decreases with inclination $\sin I$, which is especially prominent in case of the L_4 cloud. We have to admit if we compare the Eurybates family to its surroundings only ($\sin I = 0.1$ to 0.15), the difference in slopes is not so prominent. An interesting feature of the L_5 cloud is a dip in the interval $\sin I = 0.05$ to 0.1. This corresponds to the approximate location of the 1988 RG_{10} group.

The $\gamma(\sin I)$ dependence among Trojans is not unique. E.g. low-inclination bodies in the J3/2 resonance also have the SFD steeper than background ($\gamma = -2.5 \pm 0.1$ versus -1.7 ± 0.1), without any clear family and a few big interlopers. May be, this feature reflects different *source reservoirs* of low- and high-inclination bodies among Trojans and J3/2?[5]

We also test albedo distributions dependent on size, since the measurements by Fernández et al. (2009) suggested small Trojans are significantly brighter and thus smaller. Large asteroids have $p_V = 0.044 \pm 0.008$ while small $p_V = 0.12 \pm 0.06$. This is a significant change of the SFD, which occurs around the size $D \simeq 30$ km. The SFD thus becomes shallower below this size, e.g. for Eurybates we would have $\gamma = -1.6$ and for L4 Trojans $\gamma = -1.5$, so the SFD's become comparable with respect to the slope. Thought, as we stated above, for a real collisional family we expect the albedo distribution to be rather homogeneous and independent of size.

2.4 Colour and spectral data

We used the Sloan Digital Sky Survey Moving Object catalogue version 4 (SDSS-MOC4) to check the families are spectraly homogenous, as we expect. Due to a larger uncertainty in the u colour in SDSS-MOC4, we used the color

[3] Of course, we have to select a 'suitable' value of the cut–off velocity for all clusters. Usually, we select that value for which $N(v_{\rm cutoff})$ is flat. Size-frequency distribution is not very sensitive to this selection anyway.

[4] Thought the number of the Eurybates members (105) is so small that it almost does not affect the mean slope of the whole L_4 population.

[5] Both Trojan and J3/2 regions are dynamically unstable during Jupiter–Saturn 1:2 mean motion resonance, so we expect the same bodies entering Trojan region may enter J3/2.

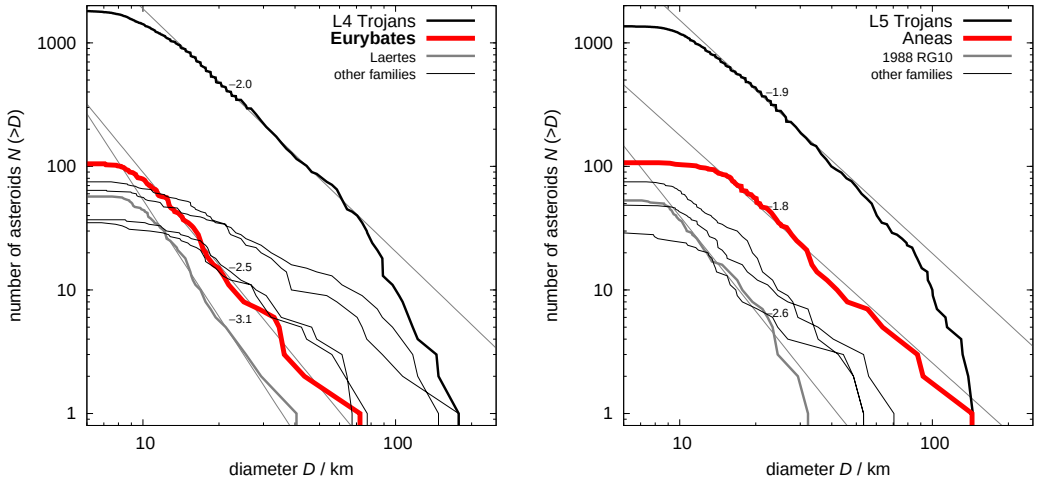

Figure 5. Left panel: size distributions of L_4 Trojans and the following clusters (there is a selected cut–off velocity in the parenthesis): Eurybates ($v_{\rm cutoff} = 50\,$m/s), Laertes (94), Hektor (160), Teucer (175), Sinon (163), 1986 WD (120). Right panel: SFD's of L_5 Trojans and the following clusters: 1988 RG_{10} (at $v_{\rm cutoff} = 130\,$m/s), Aneas (150), Asios (155), Panthoos (130), Polydoros (130).

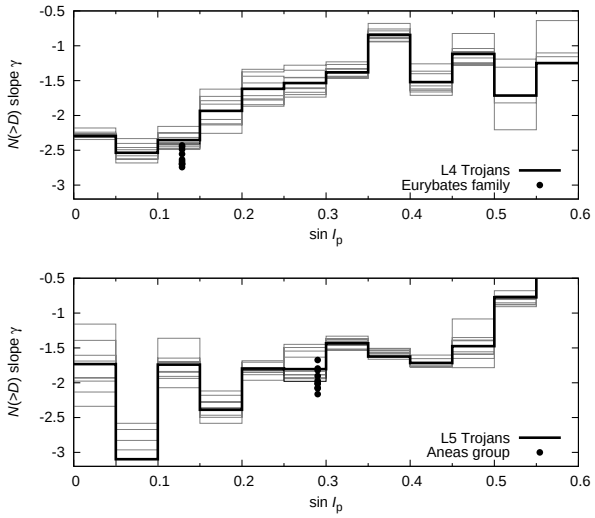

Figure 6. Slopes γ of the size-frequency distributions $N(>D)$ for L_4 and L_5 Trojans and their dependence on the inclination $\sin I$. The range of diameters for which the SFD's were fitted is $D_{\rm min} = 12\,$km, $D_{\rm max} = 30\,$km. This lines were calculated for different ranges, which were varied as $D_{\rm min} \in (10, 15)\,$km, $D_{\rm max} \in (20, 40)\,$km. Their spread indicates the uncertainty of γ in a given interval of $\sin I$.

indices a^* and $i-z$, where $a^* = 0.89(g-r)+0.45(r-i)-0.57$ (defined by Parker et al. 2008).

The result is shown in Figure 7. It is clearly visible that the distribution of the Eurybates family in the space of $(a^*, i-z)$ colours is different from the Trojan backround. On contrary, the 1988 RG_{10} group covers essentially the same area as the background. The Aneas is only slightly shifted towards larger a^* and $i-z$ with respect to the background. There is a lack of data for the Ennomos family — three bodies are not sufficient to compare the colour distributions.

Alternatively, we may use principal component analysis of the SDSS colour indices. We use only data with uncertainties smaller than 0.2 mag, which resulted in 70 887 records. We calculated eigenvalues ($\lambda_{1,2,3,4} = 0.173$, 0.0532, 0.0249, 0.0095), corresponding eigenvectors and constructed the following three principal components (Trojanová 2010):

$$\begin{aligned} {\rm PC}_1 &= 0.235\,(u-g) + 0.416\,(g-r) + 0.598\,(g-i) \\ &\quad + 0.643\,(g-z)\,, \qquad (1) \\ {\rm PC}_2 &= 0.968\,(u-g) - 0.173\,(g-r) - 0.147\,(g-i) \\ &\quad - 0.106\,(g-z)\,, \qquad (2) \\ {\rm PC}_3 &= 0.078\,(u-g) + 0.601\,(g-r) + 0.330\,(g-i) \\ &\quad - 0.724\,(g-z)\,, \qquad (3) \end{aligned}$$

which have a clear physical interpretation: $\rm PC_1$ corresponds to an overall slope, $\rm PC_2$ is a variability in the u band, and $\rm PC_3$ a depth of the 1 μm absorption band. The Eurybates family is different from Trojans in all three principal components (mean $\rm PC_1$ of the Eurybates members is smaller, $\rm PC_2$ and $\rm PC_3$ larger). The Aneas group has the same distribution of $\rm PC_2$ and $\rm PC_3$ as Trojans and the 1988 RG_{10} group is similar to Trojans even in all three components.

Hence, we confirm the Eurybates family seems distinct in color even in the fourth version of the SDSS-MOC. This fact is consistent with previous work of Roig et al. (2008), who used third version of the same catalogue and classified Eurybates family members as C-type asteroids.

Finally, note that De Luise et al. (2010) pointed out an absence of ice spectral features at 1.5 and 2.0 μm on several Eurybates members and Yang and Jewitt (2007) concluded the same for (4709) Ennomos.

2.5 Impact disruption model

We use a simple model of an isotropic disruption from Farinella et al. (1994). The distribution of velocities "at infinity" follows the function

$$\mathrm{d}N(v) = Cv(v^2 + v_{\rm esc}^2)^{-(\alpha+1)/2}\,, \qquad (4)$$

with the exponent α being a free parameter, C a normalisation constant and $v_{\rm esc}$ the escape velocity from the parent

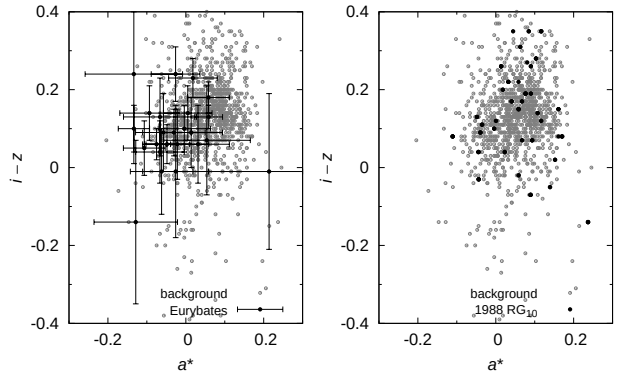

Figure 7. Left panel: The $(a^*, i-z)$ colours for the L_4 Trojans (gray dots) and the Eurybates family (black dots with error bars). The distributions differ significantly in this case. Right panel: A similar comparison for the L_4 Trojans and the 1988 RG_{10} group, which seem to be indistinguishable.

body, which is determined by its size $R_{\rm PB}$ and mean density $\rho_{\rm PB}$. The distribution is cut at a selected maximum allowed velocity $v_{\rm max}$ to prevent outliers. The orientations of velocity vectors in space are assigned randomly. We assume the velocity of fragments is independent on their size.

There are several more free parameters, which determine the initial shape of the family in the space of proper elements: initial osculating eccentricity $e_{\rm i}$ of the parent body, initial inclination $i_{\rm i}$, as well as true anomaly $f_{\rm imp}$ and argument of perihelion $\omega_{\rm imp}$ at the time of impact disruption.

An example of a synthetic family just after disruption and its comparison to the observed Eurybates family is shown in Figure 8. Usually, there is a significant disagreement between this simple model of impact disruption and the observations. Synthetic families usually look like thin 'filaments' in the $(d, e, \sin I)$ space, which are curved due to the mapping from osculating elements to resonant ones. On the other hand, observed groups among Trojans are much more spread. However, this only indicates an importance of further long-term evolution by chaotic diffusion and possibly by planetary migration.[6]

In case of the Ennomos family members, they are distributed mostly on larger semimajor axes than (4709) Ennomos, thought isotropic impact disruptions produce fragments distributed evenly on larger and smaller a. May be, it is an indication of an anisotropic velocity field? Or a different parent body of this cluster?

2.6 Planetary migration

If asteroid families are very old, planetary migration might influence their current shape. In order to study of late stages of planetary migration, which is caused by interactions with a planetesimal disk, we construct the following model. We treat the migration analytically within a modified version of the numerical symplectic SWIFT-RMVS3 integrator (Levison & Duncan 1994), which accounts for gravitational perturbations of the Sun and four giant planets and includes also an energy-dissipation term, as described in Brož et al. (2010). The speed of migration is characterised by the exponential time scale $\tau_{\rm mig}$ and the required total change of semimajor axis $a_{\rm i} - a_{\rm f}$. We use an eccentricity damping formula too, which simulates the effects of dynamical friction and prevent an unrealistic increase of eccentricities (Morbidelli et al. 2010). The amount of damping is determined by the parameter $e_{\rm damp}$.

We try to adjust initial orbital parameters of planets and the parameters of migration in such a way to end up at currently observed orbits. The integration time step is $\Delta t = 36.525$ days and the time span is usually equal to $3\tau_{\rm mig}$, when planetary orbits almost stop to migrate.

2.7 Inefficient Yarkovsky/YORP effect

On long time scales, the Yarkovsky thermal force might cause significant perturbations of orbits. We use an implementation of the Yarkovsky thermal effect in the SWIFT N-body integrator (Brož 2006). It includes both the diurnal and seasonal variants.

The YORP effect (thermal torques affecting spin states; Vokrouhlický et al. 2006) was not taken into account in our simulations. The reason is that the respective time scale $\tau_{\rm YORP}$ is of the order 100 My to 1 Gyr So as a 'zero' approximation, we neglect the YORP effect on these "short" time scales and keep the orientations of the spin axes fixed.

For Trojan asteroids captured in a 0th-order mean motion resonance, the Yarkovsky perturbation only affects the position of libration centre (Moldovan et al. 2010). Note that the perturbation acts 'instantly' — there is no systematic secular drift in eccentricity nor in other proper elements which is an important difference from 1st-order resonances, where a e-drift is expected (Brož & Vokrouhlický 2008, Appendix A). This is another reason we do not need a detailed YORP model here.

The thermal parameter we use are reasonable estimates for C/X-type bodies: $\rho_{\rm surf} = \rho_{\rm bulk} = 1300\,{\rm kg/m^3}$ for the surface and bulk densities, $K = 0.01\,{\rm W/m/K}$ for the surface thermal conductivity, $C = 680\,{\rm J/kg}$ for the heat capacity, $A = 0.02$ for the Bond albedo and $\epsilon_{\rm IR} = 0.95$ for the thermal emissivity.

3 ASTEROID FAMILIES AND INSIGNIFICANT GROUPS

In this section, we briefly discuss properties of selected clusters: Eurybates, Ennomos, Aneas and 1988 RG_{10}. We focus on these four clusters, since they seem most prominent according to our previous analysis.

3.1 Eurybates family

The Eurybates family can be detected by the hierarchical clustering method for cut–off velocities $v_{\rm cutoff} =$ 38 to 78 m/s, when it merges with Menelaus (see Figure 3). Yet, we do not rely just on the HCM! Another selection criterion we use is a 'meaningful' shape of the family and its changes with respect to $v_{\rm cutoff}$. A very important characteristics of the Eurybates family at low values of $v_{\rm cutoff}$ is a tight confinement of inclinations ($\sin I$ within 0.01). It breaks down at $v_{\rm cutoff} \simeq 68\,{\rm m/s}$, so we consider this value

[6] Only very young clusters like the Karin family (Nesvorný et al. 2002) exhibit this kind of a 'filament' shape.

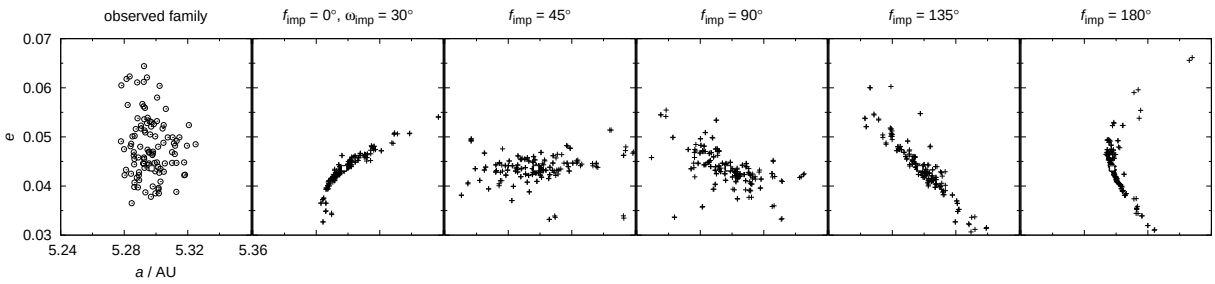

Figure 8. A comparison between the observed Eurybates family (open circles) and synthetic families (crosses) just after the impact disruption computed for several values of $f_{\rm imp} = 0°, 45°, 90°, 135°, 180°$ and $\omega_{\rm imp} = 30°$, $R_{\rm PB} = 47\,{\rm km}$, $\rho_{\rm PB} = 1300\,{\rm kg/m^3}$. Different geometry in f, ω produces a slightly different cluster, nevertheless, it is always tighter than the observed family. The position of the asteroid (3548) Eurybates is denoted by a square.

as an upper limit. The Eurybates family is also confined in semimajor axis, being approximately twice smaller than other groups.

The diameter of the parent body is $D_{\rm PB} \doteq 97\,{\rm km}$ for albedo $p_V = 0.055$ if we sum the volumes of the known bodies. Of course, in reality it is slightly larger due to observational incompleteness. If we prolong the slope of the SFD $\gamma = -2.5$ down to zero we obtain $D_{\rm PB} \doteq 110\,{\rm km}$. The geometric method of Tanga et al. (1999) gives an upper limit $D_{\rm PB} \simeq 130\,{\rm km}$.

Spectral slopes of family members are rather homogeneous and correspond to C/P-types (Roig et al. 2008).

3.2 Ennomos family

The cluster around (4709) Ennomos can be recognised for a wide interval of cut–off velocities $v_{\rm cutoff} \in (69, 129)\,{\rm m/s}$ when it stays compact and confined in inclinations ($\sin I = 0.451$ to 0.466). Very probably, there are several interlopers, because we can count 4 to 10 asteroids in the surroundings, i.e., in the same volume of the $(d, e, \sin I)$ space (see Figure 9). Since small bodies dominate the Ennomos family we suspect large bodies might be actually interlopers.

A very intriguing feature is a high albedo of (4709) Ennomos $p_V \simeq 0.15$ measured by Fernández et al. (2003). Apart from other explanations, the authors speculated it may result from a recent impact which covered the surface with pristine ice. If true the relation between the fresh surface and the collisional family might be a unique opportunity to study cratering events.

We cannot exclude a possibility that (4709) Ennomos is actually an interloper and the family is not related to it at all. Nevertheless, our hypothesis is testable: family members should exhibit a similarity in spectra and albedos. The only information we have to date are SDSS colours for three members: 98362, 2005 YG_{204} are probably C-types and 2005 AR_{72} is a D-type. In case new data become available we can remove interlopers from our sample and improve our analysis.

The size distribution of the Ennomos family is barely constrained, since small bodies are at the observational limit. Moreover, removal of interlopers can change the SFD slope completely (from $\gamma = -1.4$ to -3.2 or so). The minimum parent body size is about $D_{\rm PB} \simeq 67\,{\rm km}$ if all members have high albedo $p_V = 0.15$.

3.3 Group denoted Aneas

The Aneas group looks like a middle portion of the L_5 cloud with approximately background density. It spans whole range of semimajor axes, as background asteroids do.

The minimum size of a hypothetical parent body is $D_{\rm PB} = 160$ to $170\,{\rm km}$ (for albedo $p_V = 0.055$ to 0.041). This size is very large and an impact disruption of such body is less probable (see Section 4.4). The size-frequency distribution is shallow, with approximately the same slope as background.

According to Roig et al. (2008) the colours are rather homogeneous and correspond to D-types, with $\simeq 10\,\%$ of probable interlopers.

3.4 Group denoted 1988 RG_{10}

The group around asteroid (11487) 1988 RG_{10} again looks like a lower portion of the L_5 cloud at low inclinations, with $\sin I \in (0.06, 0.1)$. The SFD is steeper ($\gamma = -2.6 \pm 0.1$) than surroundings in L_5 and the resulting parent body size $D \simeq 60\,{\rm km}$ is relatively small. The colours seems heterogeneous (Roig et al. 2008) and we can confirm this statement based on the new SDSS-MOC version 4 data.

The remaining clusters (Hektor, Teucer, Sinon, 1986 WD, Laertes, Asios, Polydoros, Panthoos, etc.) may be characterised as follows: (i) they have a density in $(d, e, \sin I)$ space comparable to that of background (surroundings); (ii) when identified by the HCM their semimajor axes span the whole range of Trojan region; (iii) the slopes of their SFD's are comparable to the background; (iv) they are often inhomogeneous with respect to colours (according to Roig et al. 2008). These reasons lead us to a conclusion that these clusters are not necessarily real collisional families.

4 LONG-TERM EVOLUTION OF TROJAN FAMILIES

4.1 Evolution due to chaotic diffusion

We try to model long-term evolution of the Eurybates family. At first, we generate a synthetic family (consisting of 42 bodies) by an impact disruption of the parent body with required size. Then we integrate the synthetic family and compare it at particular time to the observed Eurybates family. The time span of the integration is 4 Gyr.

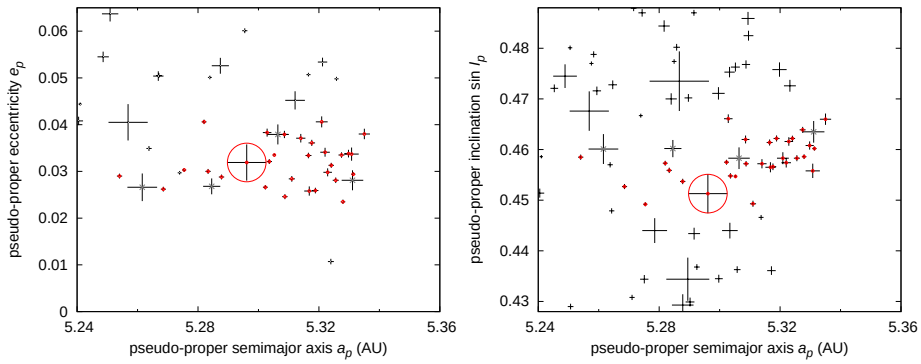

Figure 9. A detail of the L_5 Trojan population where the Ennomos family is visible. Left panel: resonant semimajor axis a vs eccentricity e. Only asteroids occupying the same range of inclinations as the Ennomos family $\sin I \in (0.448, 0.468)$ are plotted to facilitate a comparison with the density of surroundings space (background). The sizes of plus signs are proportional to diameters of the asteroids. Probable family members are denoted by small red circles and probable interlopers by small grey crosses. Right panel: a vs inclination $\sin I$, with range of eccentricities $e \in (0.02, 0.045)$.

The main driving mechanism is slow *chaotic diffusion* (the Yarkovsky effect is present but inefficient in the Trojan region). Initially, the spread of inclinations of the synthetic family is consistent with the observed one. On the other hand, the shape in (a, e) elements is clearly inconsistent.

Since the inclinations evolve only barely we focus on the evolution of in the (a, e) plane (see Figure 10). The point is the synthetic family, namely the 'filament' structure, has to disperse sufficiently. After 500 Myr it is still recognisable but after 1 Gyr of evolution it is not. So we may constrain the age of the Eurybates family from 1 to 4 Gyr.[7]

A similar analysis for the Ennomos family indicates that chaotic diffusion is faster in this region (given the large inclination) and the most probable age thus seems to be from 1 to 2 Gyr. Beyond 2 Gyr the inclinations of the synthetic family become too large compared to the observed Ennomos family, while the eccentricites are still compatible.

We try to model Aneas and 1988 RG_{10} groups too (see Figure 11). In these two cases, there is a strong disagreement between our model and observations. The observed groups are much larger and chaotic diffusion in respective regions is very slow. Even after 4 Gyr of orbital evolution, the synthetic family remains too small.

The only free parameter which may substantially change our results is the initial velocity distribution. Theoretically, the distribution might have been strongly anisotropic. However, we cannot choose initial velocities entirely freely, since their magnitude should be comparable to the escape velocity from the parent body, which is fixed by the size $D_{\rm PB}$ and only weakly dependent on a-priori unknown density $\rho_{\rm PB}$.

Another solution of this problem is possible if we assume families are very old and they experienced perturbations due to planetary migration.

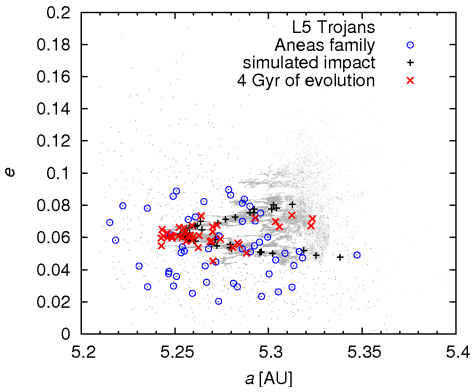

Figure 11. Evolution of the synthetic family over 4 Gyr versus the observed Aneas group. Chaotic diffusion is slow and it seems impossible to match the large spread of the observed group even after 4 Gyr.

4.2 Stability during planetary migration

The major perturbation acting on Trojans are *secondary resonances* between the libration period $P_{J1/1}$ of the asteroid in the J1/1 mean-motion resonance with Jupiter and the period P_{1J-2S} of the critical argument of Jupiter–Saturn 1:2 resonance (Morbidelli et al. 2005)

$$P_{J1/1} = nP_{1J-2S}\,, \tag{5}$$

where n is a small integer number. Typical libration periods are $P_{J1/1} \simeq 150$ yr and P_{1J-2S} changes as planets migrate (it decreases because Jupiter and Saturn recede from their mutual 1:2 resonance).[8]

All synthetic families are strongly unstable when $P_{1J-2S} \simeq 150$ yr and even during later stages of migration with $P_{1J-2S} \simeq 75$ yr the eccentricities of family members are perturbed too much to match the observed families like Eu-

[7] We verified these estimates by a 2-dimensional Kolmogorov–Smirnov test of the (a, e) distributions: initially the KS distance is $D_{\rm KS} = 0.30$ and the probability $p_{\rm KS}(>D) = 0.02$, which means the distribution are incompatible. At $t = 1$ Gyr, the values are $D_{\rm KS} = 0.20$ and $p_{\rm KS}(>D) = 0.32$, which indicates a reasonable match.

[8] Another source of instability might be a secondary resonance with P_{2J-5S} (the so called Great Inequality period) thought it is weaker than P_{1J-2S}. We find no asteroids perturbed by secondary resonances connected with P_{3J-7S} or P_{4J-9S} which are present 'en route'. Neither Uranus nor Neptune play an important role.

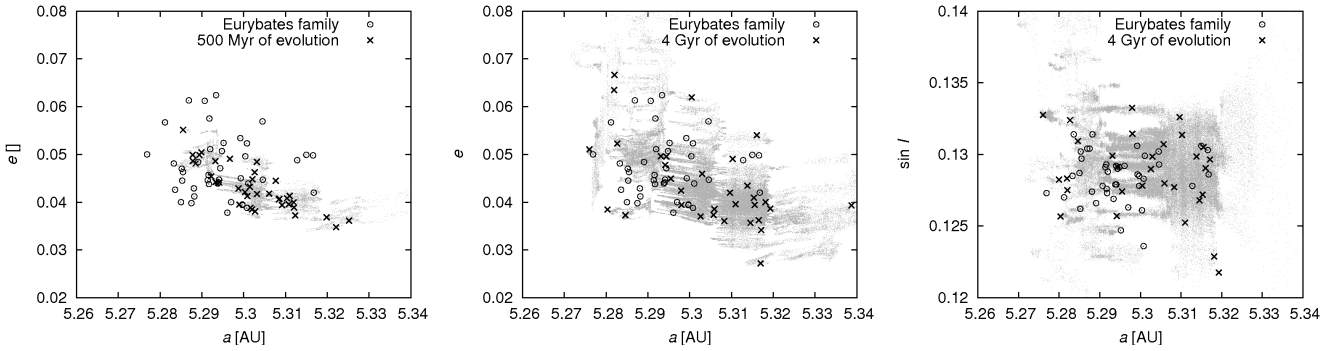

Figure 10. Orbital evolution of the synthetic family and its comparison with the observed Eurybates family. Left panel: the situation in the (a, e) plane at 500 Myr. Middle panel: the situation after 4 Gyr. Chaotic diffusion disperses the synthetic family in course of time (see shaded tracks of particles). Right panel: the $(a, \sin I)$ plane at the same time. Inclinations evolve only barely.

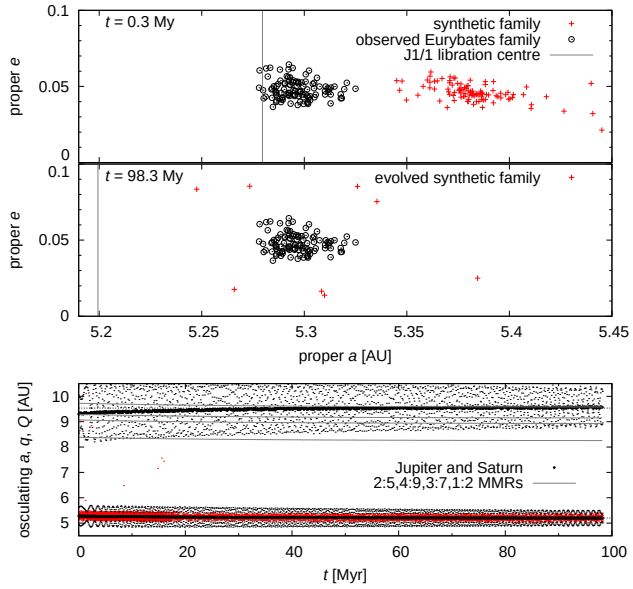

Figure 12. Evolution of a synthetic family during late phases of planetary migration ($\tau_{\rm mig} = 30$ Myr in this case). Top panel: the state at 0 Myr, middle: 100 Myr, bottom: the respective orbital evolution of Jupiter and Saturn. The family is almost destroyed and it is definitely incompatible with the observed Eurybates family.

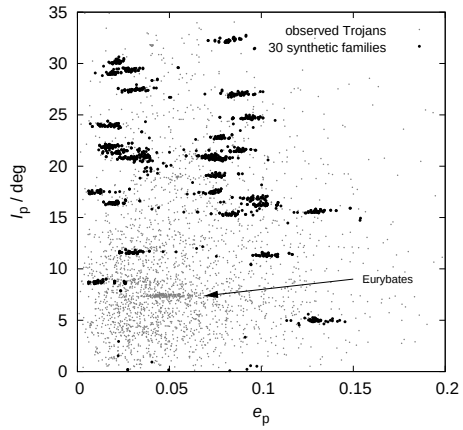

Figure 13. Proper eccentricities and inclinations of 30 *synthetic* families (black dots), which originated near the border of stable libration zone, compared to the observed L4 Trojans (gray dots).

rybates or Ennomos (see Figure 12). There are practically no plausible migration scenarios – regardless of time scale $\tau_{\rm mig}$ – which would produce a sufficiently compact group, unless Jupiter and Saturn are almost on their current orbits. We tested $\tau_{\rm mig} = 0.3, 3, 30$ Myr and even for $\Delta a_{\rm J} \equiv a_{\rm Jf} - a_{\rm Ji}$ as small as -0.08 AU and $\Delta a_{\rm S} = +0.25$ AU the perturbation was too strong. The reason is that one has to avoid $n = 2$ secondary resonance to preserve a low spread of a synthetic family.

Let us conclude if any of Trojan families was created during planetary migration and if the migration was smooth (exponential) the family cannot be visible today. Anyway, we cannot exclude a possibility that final stages of migration were entirely different, e.g., similar to the 'jumping-Jupiter' scenario (Morbidelli et al. 2010).

4.3 Families lost by ballistic transport

We studied a possibility that some families cannot be identified because the breakup occurred at the outskirts of the stable libration zone. We thus chose 30 largest asteroids near the edge of the L_4 libration zone and we simulated breakups of these asteroids which create families with 30 fragments each. We assumed the diameter of all parent bodies equal to $D_{\rm PB} = 100$ km and their density $\rho_{\rm PB} = 1.3\,{\rm g\,cm^{-3}}$. The breakups always occurred at the same geometry $f_{\rm imp} = 0°$, $\omega_{\rm imp} = 30°$. After the breakup, we calculated proper elements of the family members and plotted their distribution (see Figure 13). We can see all 30 synthetic families can be easily identified. In most cases, more than 95 % of family members remained within the stable libration zone. We can thus conclude that the ballistic transport does not affect the number of observed families among Trojans.

4.4 Collisional rates

We can estimate collisional activity by means of a simple stationary model. Trojan–Trojan collision play a major role here, because Trojans are detached from the Main Belt. In case of Eurybates, the target (parent body) diameter $D_{\rm target} = 110$ km, mean impact velocity $V_{\rm imp} = 5.20$ km/s

(Dahlgren 1998), strength $Q^\star_D = 10^5$ J/kg (it scales as D^2 in gravity regime) and thus the necessary impactor size (Bottke et al. 2005)

$$d_{\rm disrupt} = \left(2Q^\star_D/V^2_{\rm imp}\right)^{1/3} D_{\rm target} \simeq 21\,{\rm km}\,. \quad (6)$$

Number of $\geqslant$21 km projectiles among L_4 Trojans is $n_{\rm project} = 434$ and we have $n_{\rm target} = 9$ available targets. An intrinsic collisional probability for Trojan–Trojan collisions $P_{\rm i} = 5.94 \times 10^{-18}\,{\rm km}^{-2}\,{\rm yr}^{-1}$ (Dahlgren 1998) and corresponding frequency of disruptions is

$$f_{\rm disrupt} = P_{\rm i} \frac{D^2_{\rm target}}{4} n_{\rm project} n_{\rm target} \simeq 7 \cdot 10^{-11}\,{\rm yr}^{-1}\,. \quad (7)$$

Over the age of the Solar System $T_{\rm SS} \simeq 4$ Gyr (after LHB), we have a very low number of such events $n_{\rm events} = T_{\rm SS} f_{\rm disrupt} \simeq 0.23$. This number seems to be in concert with only one $D \geqslant 100$ km family currently observed among Trojans.[9]

The parent body of Aneas group is 1.5 larger and consequently the resulting number of events is more than one order of magnitude lower. On the other hand, clusters with smaller parent bodies ($D_{\rm PB} \ll 100$ km) or significantly weaker ($Q^\star_D \ll 10^5$ J/kg) might be more frequent.

During the Late Heavy Bombardment epoch we may assume a substantial increase of collisional activity (Levison et al. 2009). Hypothetical old families were however probably 'erased' due to the late phases of planetary migration (see Section 4.2) unless the migration time scale for Jupiter and Saturn was significantly shorter than the time scale of the impactor flux from transneptunian region which is mainly controlled by the migration of Uranus and Neptune.

5 CONCLUSIONS

Increasing number of Trojan asteroids with available proper elements enables us to get new insights into this important population. Essentially, new faint/small asteroids filled the 'gaps' in the proper-element space between previously known clusters and today it seems most clusters are rather comparable to background. One should be aware that the number of families among Trojans may be low and one should not take the number of $\simeq 10$ families as a rule.

Only the C-type Eurybates family fulfils all criteria to be considered a collisional family. This is probably also true for the newly discovered Ennomos family. Moreover, there might be a potentially interesting relation between the high-albedo surface of (4709) Ennomos and the collisional family thought we do not have enough data yet to prove it independently (by colours, spectra or albedos).

Note there may exist clusters among Trojans which are not of collisional origin. They may be caused by: (i) differences in chaotic diffusion rates; (ii) $a/e/I$-dependent efficiency of original capture mechanism; or (iii) it may somehow reflect orbital distribution in source regions.

We cannot exclude a hypothetical existence of old families which were totally dispersed by dynamical processes, e.g., by perturbations due to planetary migration which is especially efficient in the Trojan region.

Finally, note there seem to be no D-type families anywhere in the Solar System. May be, the D-type parent bodies are too weak and the target is completely pulverized during a collision? This might have important implications for collisional models of icy bodies.

[9] A similar stationary estimate valid for the Main Asteroid Belt gives the number of events 12 while the number of observed families with $D_{\rm PB} \gtrsim 100$ km is about 20 (Durda et al. 2007). These two numbers are comparable at least to order-of-magnitude.

ACKNOWLEDGEMENTS

We thank David Vokrouhlický, David Nesvorný, Alessandro Morbidelli and William F. Bottke for valuable discussions on the subject. We also thank Lenka Trojanová for the pricipal component analysis of the SDSS-MOC4 data. The work has been supported by the Grant Agency of the Czech Republic (grant 205/08/P196) and the Research Program MSM0021620860 of the Czech Ministry of Education. We acknowledge the usage of computers of the Observatory and Planetarium in Hradec Králové.

REFERENCES

Beaugé C., Roig F., 2001, Icarus, 153, 391
Bottke W.F., Durda D.D., Nesvorný D., Jedicke R., Morbidelli A., Vokrouhlický D., Levison H.F., 2005, Icarus, 175, 111
Brož M., Vokrouhlický D., 2008, MNRAS, 390, 715
Brož M., Vokrouhlický D., 2010, MNRAS, submitted
Dahlgren M., 1998, A&A, 336, 1056
Durda D.D., Bottke W.F., Nesvonrý D., Enke B.L., Merline W.J., Aspaugh E., Richardson D.C., 2007, Icarus, 186, 498
Farinella P., Froeschlé C., Gonczi R., 1994, in Milani A., Di Martino M., Cellino A., eds., Asteroids, comets, meteors 1993. Kluwer Academic Publishers, Dordrecht, p. 205
Fernández Y.R., Jewitt D.C., Ziffer J.E., 2009, AJ, 138, 240
Fernández Y.R., Sheppard S.S., Jewitt D.C., 2003, AJ, 126, 1536
Gomes R., Levison H.F., Tsiganis K., Morbidelli A., 2005, Nature, 435, 466
Knežević Z., Milani A., 2003, A&A, 403, 1165
Laskar J., Robutel P., 2001, Celest. Mech. Dyn. Astron., 80, 39
Levison H.F., Duncan M., 1994, Icarus, 108, 18
Levison H.F., Bottke W.F., Gounelle M., Morbidelli A., Nesvorný D., Tsiganis K., 2009, Nature, 460, 364
De Luise F., Dotto E., Fornasier S., Barucci M.A., Pinilla-Alonso N., Perna D., Marzari F., 2010, Icarus, 209, 586
Milani A., 1993, Cel. Mech. Dyn. Astr., 57, 59
Moldovan R., Matthews J.M., Gladman B., Bottke W.F., Vokrouhlický D., 2010, ApJ, 716, 315
Morbidelli A., Levison H.F., Tsiganis K., Gomes R., 2005, Nature, 435, 462
Morbidelli A., Brasser R., Gomes R., Levison H.F., Tsiganis K., 2010, AJ, accepted
Nesvorný D., Bottke W.F., Dones L., Levison H.F., 2002, Nature, 417, 720
Nesvorný D., Bottke W.F., Levison H.F., Dones L., 2003, ApJ, 591, 486

Nesvorný D., Vokrouhlický D., Bottke W.F., 2006, Science, 312, 1490
O'Brien D., Morbidelli A., 2008, LPI Cont., 1405, 8367O
Parker A., Ivezić Ž., Jurić M, Lupton R., Sekora M.D., Kowalski A., 2008, Icarus, 198, 138
Quinn T.R., Tremaine S., Duncan M., 1991, AJ, 101, 2287
Roig F., Ribeiro A.O., Gil-Hutton R., 2008, A&A, 483, 911
Szabó Gy.M., Ivezić Ž., Jurić M, Lupton R., 2007, MNRAS, 377, 1393
Šidlichovský M., Nesvorný D., 1997, Celest. Mech. Dynam. Astron., 65, 137
Tanga P., Cellino A., Michel P., Zappalà V., Paolicchi P., Dell'Oro A., 1998, Icarus, 141, 65
Trojanová L., 2010, Bc thesis, Univ. Hradec Králové
Yang B., Jewitt D., 2007, AJ, 134, 223
Zappalà V., Cellino A., Farinella P., Milani A., 1994, AJ, 107, 772

This paper has been typeset from a TEX/ LATEX file prepared by the author.